

THE DYNAMIC AND EARTHQUAKE RESPONSE OF BASILICA CHURCHES IN KEFALONIA, GREECE INCLUDING SOIL- FOUNDATION DEFORMABILITY AND WALL DETACHMENT.

G.C. Manos¹, E. Kozikopoulos²

¹ Professor and Director of the Lab. of Strength of Materials and Structures, Aristotle University
e-mail: {gcmayos@civil.auth.gr}

² Postgraduate student, Lab. of Strength of Materials and Structures, Aristotle University
e-mail: {vago_kozi@outlook.com.gr}

Keywords: Christian churches, Numerical simulation, Dynamic and seismic response, Soil-foundation deformability, detachment of walls, push-over non-linear analyses

Abstract. *The dynamic and earthquake behaviour of structural systems representing Post-Byzantine Christian churches located in Kefalonia-Greece is examined. All these churches are made of stone masonry. They developed damage to their masonry elements due to the amplitude of the gravitational forces acting together with the seismic forces that were generated by the recent 2014 earthquake activity, combined with the deformability of the foundation. The numerical results together with assumed strength values are utilized to predict the behaviour of the various masonry parts of these churches in in-plane, shear, and normal stress as well as out-of-plane flexure. Use is made in the numerical simulation of the deformability of the foundation of the results obtained from a specific investigation that dealt in measuring the dynamic characteristics of a bell tower located in Lixouri-Kefalonia-Greece. It is shown that the foundation deformability partly explains the appearance of structural damage. When comparing the numerically predicted regions that reach limit state conditions with actual damage patterns a reasonably good agreement in a qualitative sense can be observed. In addition, the numerical simulation focused in reproducing numerically certain non-linear mechanisms that are typical for this type of structural systems. The numerically predicted non-linear response mechanisms at the corners of the masonry walls as well as at the roof to masonry wall level seem to reproduce in a realistic way the observed damage patterns in these regions.*

1 INTRODUCTION

The objective of this paper is to study the dynamic and earthquake behavior of Christian churches of the Basilica typology in the island of Kefalonia, Greece (figure 1). The recent devastating earthquake activity in the island during the period from 26th of January till the 3rd of February 2014 caused extensive damage to the masonry walls of many of these structures. The worst hit region lies at the West part of the island of Kefalonia with the peninsula of Paliki claiming the biggest share of damaged churches. This region is marked in figure 1 with the dotted circle. The most damaging seismic event for this region was the ground motion during the major aftershock of this earthquake sequence that occurred during the 3rd of February, 2014 [1, 2, 3, 4]. This is depicted in figures 2 and 3. Figure 2 shows the location of the epicenters of the aftershocks of the earthquake sequence of January-February 2015 for the island of Kefalonia, including the epicenter of the strongest aftershock of 3rd February, 2015 [2]. Figure 3 marks the location of some of the various churches in the Paliki peninsula that were shaken by this strongest aftershock, leading to considerable damage and to certain cases to spectacular partial collapse (figures 4 and 5).

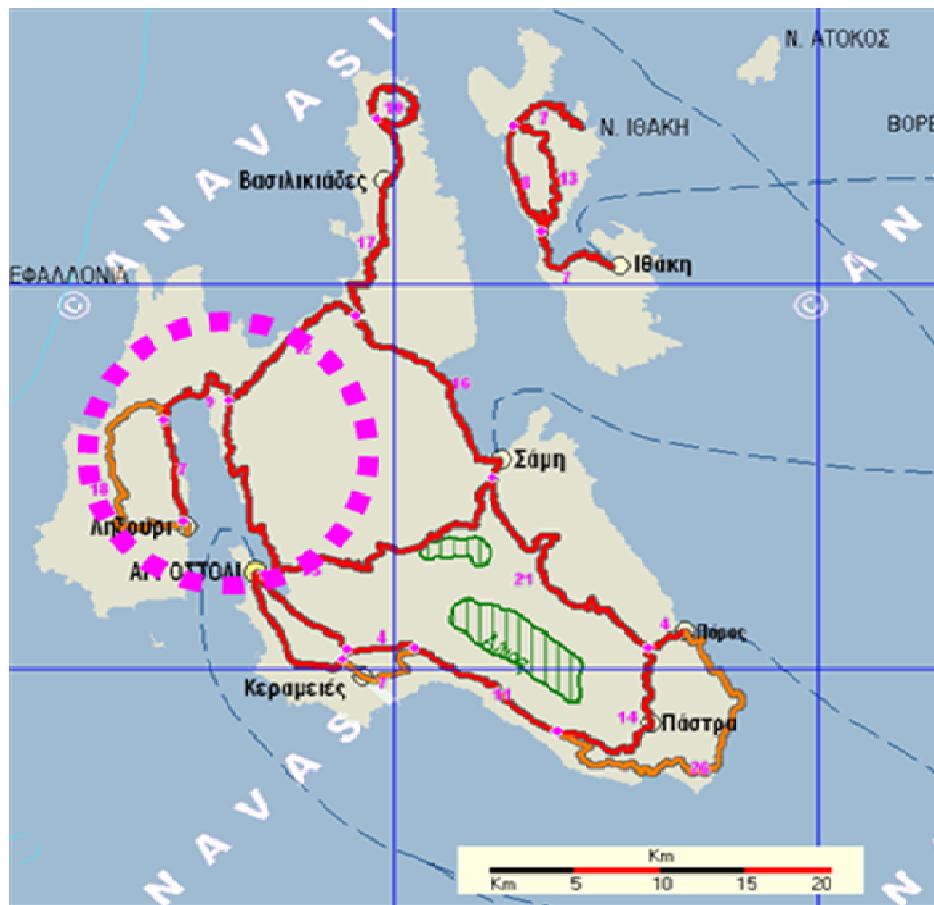


Figure 1. View of the island of Kefalonia, Greece together with the peninsula of Paliki

The main event of this earthquake sequence occurred on the Sunday, 26th of January 2015, 13:55 local time [1]. Fortunately, this event was not so damaging for the churches and despite the fact that it occurred Sunday the Christian services were already completed by that time. The damaging aftershock occurred on the Monday of 3rd February 2015, local time 05:09. The fact that at this time the churches were empty companioned with the warning of the

preceded main event are factors that helped to have no loss of life from the structural damage and partial collapse that was observed in certain churches as well as to a number of other structures and facilities ([1, 2, 3]).

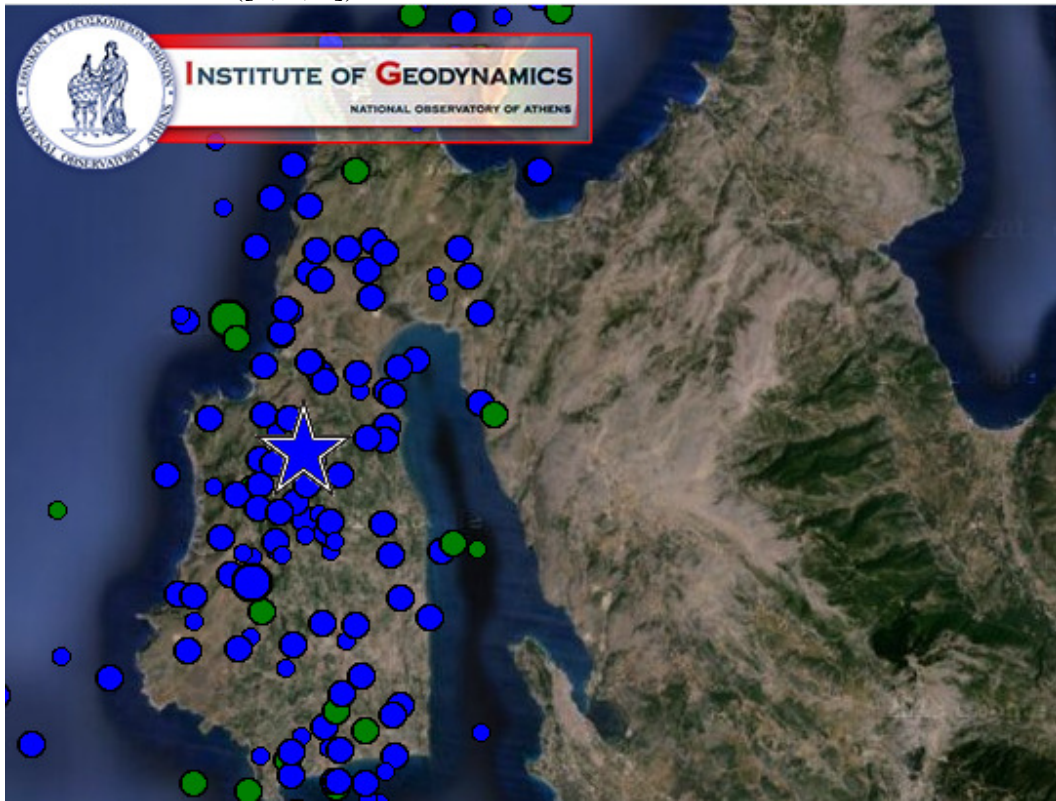


Figure 2. View of the epicenters of the aftershocks together with that of the strongest aftershock of 3rd of February, 2015 (blue star) as they were recorded by the Institute of Geodynamics of the National Observatory of Athens, Greece.



Figure 3. View of peninsula of Paliki together with the location of some of the churches that developed structural damage during the strongest aftershock of 3rd February, 2015.



Figure 4. Virgin Mary of Roggoi



Figure 5. St. Marina Soullaroi

During the Frankish and Venetian periods in Kefalonia many churches of this typology were rebuilt in Kefalonia. Indicatively, around the late 18th century there were 350-400 churches in this beautiful island of the Ionian sea with the very active geological seismic background. Numerous churches in this island have the structural form the single aisle basilica (Ionian) with an elongated rectangular shape. The value of the ratio of their longitudinal length over the transverse length varies from 1: 1.5 for relatively small churches to 1: 5 for the largest structures. This relatively simple structural system for these churches is formed by load-bearing stone-masonry peripheral walls that are connected with well built corners as well as by the presence of a soft system of trusses that form the lightweight roof. Table 1 lists a number of churches that were affected by this earthquake sequence together with the century of their construction as well as the century of their damage repair due to a previous earthquake activity [3]. The island of Kefalonia belongs to a high seismic hazard region, as this is depicted by the map of seismic zones of Greece in figure 6. This seismic zonation is included in the current seismic code of Greece[26]; it can be seen in this figure that the island of Kefalonia belongs to the seismic zone having seismic design ground acceleration value equal to 0.36g (g the acceleration of gravity equal to 9.81m/sec. However, it must be pointed out that this is a relatively recent regulation that does not apply to the construction methods of the 17th century.

Table 1. The name of the studied churches and the century of construction and repair.

A/A	name of church	Century of Construction / Repair
1	Kechrionos Monastery	17 th / 20 th
2	Virgin Mary Kontogennada	18 th / 20 th
3	St. Thekla	17 th / 20 th
4	Virgin Mary Damoulianouta	19 th / 20 th
5	Virgin Mary of Roggoi	17th
6	Virgin Mary Dematora	19 th / 20 th
7	St. Blaise Dematora	18 th
8	St. Dimitrios Kalata	18 th / 20 th
9	Birth of the Virgin Mary Kalata	18 th
10	12 Apostles -Chavdata	19 th
11	Birth of the Virgin Mary Havriata	17 th / 20 th
12	St. Marina in Soullaroi	17th

* The repair for the 20th century refers to interventions introduced after the damaging 1953 earthquake sequence



Figure 6. The location of the six most damaged urban areas of Greece from the earthquake activity during the last thirty years together with the seismic zoning map (see also Tables 1 and 5).

Damage to Christian churches from earthquake activity in Greece is quite frequent [6 to 21]. This must be attributed to the intense earthquake activity and the accumulation of damage as well as to the fact that such structures made of weak masonry are quite vulnerable as their heavy walls and heavy elements in their superstructure results in large amplitude earthquake demands that cannot be met by the resistance offered by relatively weak stone masonry structural elements [6]. This is also the case in the damaged churches of Kefalonia that will be investigated in the following sections.



Figure 7. Peninsula of Paliki with the location of the two churches being examined here

It should be underlined here that neither the long history of intense seismic activity in the island nor the attempted damage repair from previous earthquake activity (see table 1) were able to create effective interventions that would protect these structures from future seismic

events. As can be seen in table 1 most of the repair efforts are dated on the 18th century. The objective of this paper is to present currently available scientific tools that can help understand the earthquake behaviour of this type of structures and therefore serve the objective of their protection in a possible more effective way than the experience of the current earthquake damage indicates. As indicated in table, the 20th century repair effort refers to interventions introduced to these churches after the damaging 1953 earthquake sequence. In general, typical interventions in these churches included the construction of a reinforced concrete beam at the top of the masonry wall to connect the wooden roof at this level. However, as the full details of these interventions were not available their effectiveness in the observed performance is so far non-conclusive.

This investigation presents the evaluation of two Christian Basilica churches that are indicated with relatively large letters in Table 1. The first is the church of Virgin Mary of Roggoi (No 5 in Table 1) and the second is church of St. Marina in Soullaroi (No 12 in Table 1 and figure 4). Both these churches are structure that did not experienced any interventions after the 1953 earthquake sequence. The first church of Virgin Mary of Roggoi has dimensions in plan 7.5m by 15.8m and a height of 9.3m (No 5 in Table 1) and the second church of St. Marina in Soullaroi has dimensions in plan 9.5m by 22.3m and a height of 9.6m, a somewhat larger structure. The investigation being conducted here includes the effects of foundation deformability [21]. It has been demonstrated in the past [17, 19, 22, 23] as well as in two companion works that are presented in this conference [22, 23], that the foundation deformability is a significant parameter in the effort to understanding the earthquake behaviour of these structures. The location of these two churches in the Paliki peninsula is shown in figure 7 together with the location of the accelerographs that recorded the seismic ground motion during the strongest aftershock of 3rd of February, 2015. Use of this recorded ground motion will be made in the framework of the current investigation.

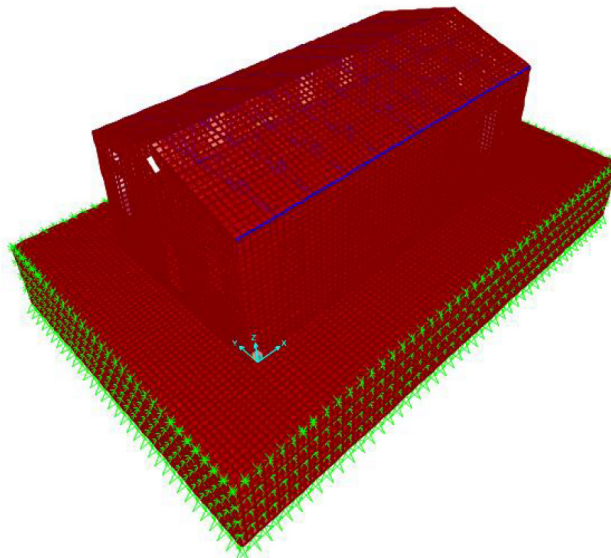


Figure 8. Numerical model of the foundation slab and the underlying soil.

2 SOIL – FOUNDATION DEFORMABILITY

The foundation of both churches is considered to be formed by a peripheral masonry strip that is an extension of the masonry walls in the sub-soil at a depth of 0.5 m. In-situ studies that were performed with the Agios Gerasimos bell tower have demonstrated that certain in-

fluences can arise on the dynamic and earthquake response from soil-foundation deformability [22, 23] that should be investigated. In order to study numerically the soil-foundation deformability of these two churches the following process was utilized.

First, a numerical model of the structure and the masonry foundation strip was formed as shown in figure 8. Together with the foundation masonry strip, which was modeled with shell elements having linear elastic properties based on the Young's modulus of masonry, the soil layers underneath were also modeled being in full contact with the masonry foundation. These soil layers were formed with solid "brick" type finite elements with linear elastic properties that extended to a depth of 4m below the foundation – soil interface.

Because it was not possible to find reliable geotechnical data in the vicinity of the studied structures the investigation of the soil-foundation deformability was attempted in a parametric way as will be explained below in order to define the elastic properties of the soil elements.

1st case. A shear wave velocity equal to 419m/sec was assumed for these underlying soil layers. This value, together with a soil density equal to 20KN/m³ leads to a shear modulus equal to 354MPa. This value together with a Poisson's ratio value equal to 0.2 leads to a Young's modulus value for the soil equal to 1000MPa. This represents a rather hard soil.

2nd case. Following the same rational but this time assuming a shear wave velocity value equal to 200m/sec leads for the same value of soil density as in the 1st case to a the Young's modulus value for the soil equal to 230MPa. This represents a medium stiffness soil and is comparable with the corresponding value found from the Agios Gerasimos in-situ measurements [22].

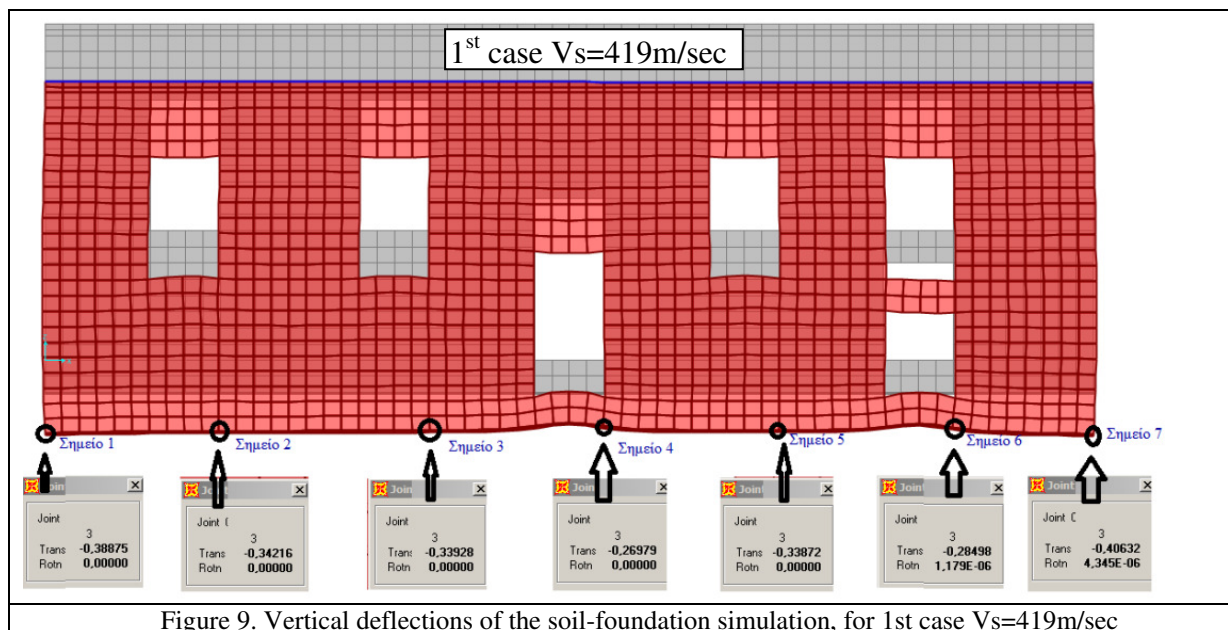


Figure 9. Vertical deflections of the soil-foundation simulation, for 1st case $V_s=419\text{m/sec}$

Next, this numerical simulation that included the superstructure, the foundation masonry strip and the soil layers, as described before, was subjected to the dead weight. The bottom surface of the bottom layer of the soil volume was constrained to have zero displacements in all three directions. The side boundaries of the soil volume were constrained only in the two horizontal directions. In this way the foundation was displaced almost uniformly downwards in the vertical direction being compressed in this way. Figures 9 and 10 depict the resulting vertical deformation patterns of the foundation-soil interface for the 1st ($V_s=419\text{m/sec}$) and 2nd ($V_s=200\text{m/sec}$) case of soil deformability, respectively.

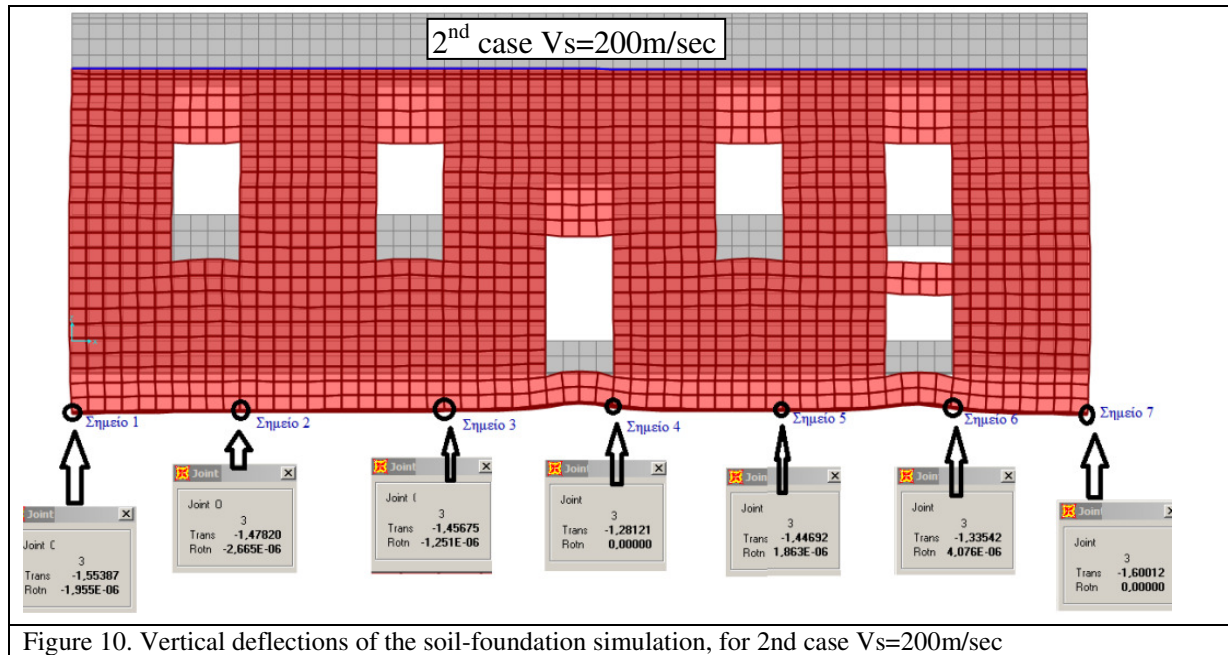


Figure 10. Vertical deflections of the soil-foundation simulation, for 2nd case Vs=200m/sec

In order to simplify the final numerical model of the examined churches including the soil-foundation deformability the following approximation was made. An alternative numerical model of the foundation masonry strip – soil interface was formed. This model retained all the aspects of the superstructure and the foundation masonry strip. However, this time the soil layers being simulated before with solid brick elements were replaced with two-node 3-D link elements having one node fully restrained in the all three directions as the support to the earth and the other node in full contact with each node of the shell elements which simulate the bottom surface of foundation masonry strip. Moreover, these two-node links were given such an axial stiffness that when the same load was applied as before (Dead load) the resulting vertical deflection of the bottom surface of the foundation – soil interface was as close as possible to the values indicated before in figures 8 and 10. Moreover, for certain types of numerical analyses a non-linearity was introduced in the axial direction of these two-node link elements resulting in their inability to sustain any tension. Following this rational the axial stiffness of these two-node link elements, utilized for case 1 and 2 of soil-foundation deformability, is listed in the following table 2.

Table 2. Axial stiffness of the equivalent two-node links

Soil deformability	1 st case Vs=419m/sec	2 nd case Vs=200m/sec
Axial Stiffness of the vertical two-node links (KN/mm)	109	24.5

3 THE LINEAR DYNAMIC RESPONSE OF THE CHURCHES

The eigen-modes and eigen-periods of the two temples are investigated next in a parametric way, assuming linear elastic behaviour of all the elements of the superstructure as well as the foundation links [21]. The following parameters are varied:

a1) The church of the **Panagia (Virgin Mary) of Roggoi**. It is one of the oldest -along with Ag. Marina in Soullaroi- Christian churches that developed severe damage during the recent earthquake. It is a relatively small church with heavy structural damage in the façade (West side) and wide shear cracks in the longitudinal North (figure 12) and South walls.



Figure 11: West side



Figure 12 North side

a2) The church of **Agia Marina** is located in **Soullaroi** and was built in the 17th century, without being repaired in 1953. It has old type double stone masonry walls, which sustained heavy damage. There is almost partial collapse of the East (figure 5) and West side (figure 13) and a wide detachment of the longitudinal and transverse walls (figure 14). very crosswise shear cracks in columns. There is also global failure of the east pediment and intense horizontal cracks appear at the base of the west.



Figure 13: West side



Figure 14 South-East corner

In all these linear elastic simulations of the dynamic response the soil-foundation deformability was approximated in the way described in section 2. That is a 1st case is examined having vertical two-node links at the soil-foundation slab interface with axial stiffness equal to 109KN/mm, representing relatively hard soil conditions. Then, a 2nd case is examined having vertical two-node links at the soil-foundation slab interface with axial stiffness equal to 24.5KN/mm, representing a soil of medium deformability. Moreover, in all cases the vertical walls were connected at the corners with two-node 3-D links in an effort to control the rigidity of these connections as well as to approximate the structural behaviour when the examined structures exhibited heavy damage in these locations.

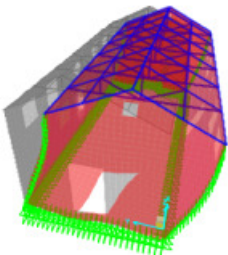
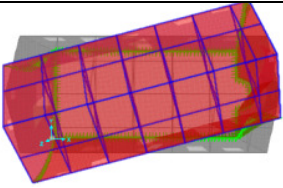
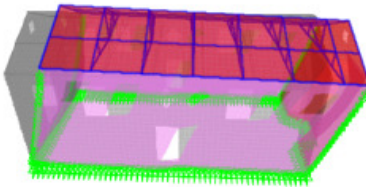
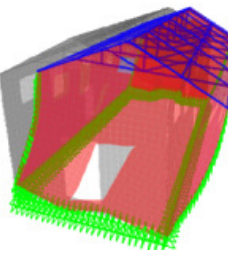
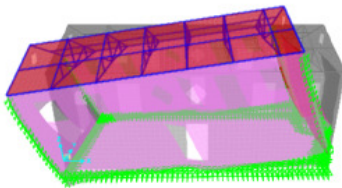
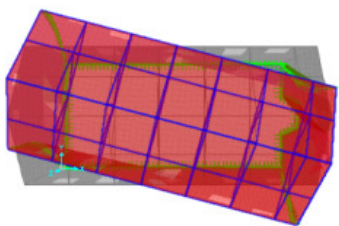
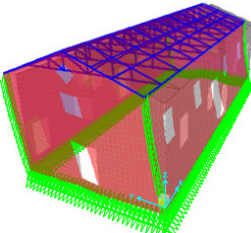
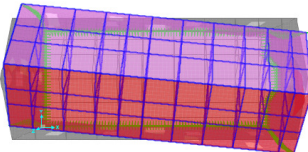
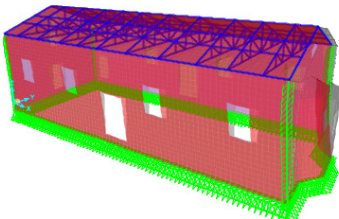
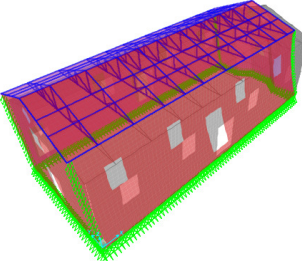
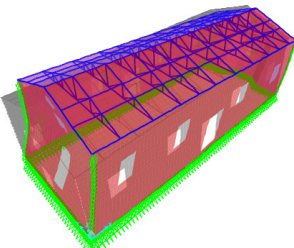
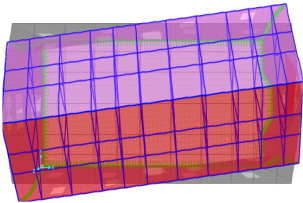
Figure 15	Panagia (Virgin Mary) of Roggoi Soil-Foundation deformability eigen-period T		
	T ₁	T ₂	T ₃
1 st case hard soil	 <p>T1y=0.1773sec mx = 0.0% my = 77.9%</p>	 <p>T2=0.1051sec mx = 0.4% my = 79.3%</p>	 <p>T3x=0.1025sec mx = 72.8% my = 79.3%</p>
2 nd case Soft soil	 <p>T1y=0.2014sec mx = 0.0% my = 75.3%</p>	 <p>T2x=0.1196sec mx = 60.6% my = 75.3%</p>	 <p>T3=0.1086sec mx = 60.6% my = 76.0%</p>

Figure 16	Agia Marina in Soullaroi - Soil-Foundation deformability 2 nd eigen-period T2		
	T ₁	T ₂	T ₃
1 st case hard soil	 <p>T1y=0.1786sec mx = 0.0% my = 80.3%</p>	 <p>T2=0.1109sec mx = 6.8% my = 80.4%</p>	 <p>T3x=0.1088sec mx = 74.2% my = 80.4%</p>
2 nd case Soft soil	 <p>T1y=0.1975sec mx = 0.0% my = 77.4%</p>	 <p>T2x=0.1206sec mx = 64.6% my = 77.4%</p>	 <p>T3=0.1133sec mx = 65.2% my = 77.5%</p>

The results of this dynamic analyses in terms of eigen-modes, eigen-period values and values of the corresponding mass participation ratios are included in figures 15 and 16 for the church of Panagia of Roggoi and Agia Marina of Soularroi, respectively ([7 to 21]).

The following remarks can be made on the basis of the results presented in these figures.

1) The first dominant eigen-mode for both churches and for both cases of foundation-soil flexibility is the translational mode in the North-South direction (y-y). The eigen-period for this mode varies from approximately 0.18sec (hard soil) to 0.20sec. (medium soil) for both churches. This eigen-mode mobilizes in all cases approximately 75% to 80% of the total mass.

2) The second dominant mode in the case of hard soil conditions is a torsional mode. The eigen-period for this mode is approximately 0.11sec for both churches. However, this mode mobilizes very little mass.

3) The third dominant mode in the case of hard soil is the translational mode in the East-West direction (x-x). The eigen-period for this mode is approximately 0.10sec. for both churches. This eigen-mode mobilizes for both churches approximately 70% of the total mass.

4) The second dominant mode in the case of medium soil conditions is the translational mode in the East-West direction (x-x). The eigen-period for this mode is approximately 0.12sec. for both churches. This eigen-mode mobilizes for both churches approximately 60% of the total mass. In the case of medium soil the third dominant mode is a torsional mode. The eigen-period for this mode is approximately 0.11sec for both churches. However, this mode mobilizes again very little mass.

From the above remarks it can be concluded that the assumed variation of the soil-foundation deformability results, as expected, in a modest increase in the fundamental eigen-period values. Moreover, the increased soil-foundation deformability results in the two translational North-South (x-x) and East-West (y-y) eigen modes becoming the dominant eigen-modes of the structural response for these churches mobilizing 75% and 60% of the total mass, respectively.

4 PREDICTIONS OF THE EARTHQUAKE RESPONSE FOR THE POST-BYZANTINE CHRISTIAN CHURCHES

Next, numerical simulations of the earthquake response of these two churches are presented. The numerical analyses that were performed towards obtaining earthquake response predictions of such Christian Basilica churches fall in the following two main categories.

4.1 Static numerical analyses with linear mechanisms for the two-node links at the foundation-soil interface as well as at the corner of masonry wall interconnections.

In these dynamic numerical analysis use will be made of the ground acceleration that was recorded at two stations during the 3rd of February strongest aftershock [1, 3]. As can be seen in figure 7, the location of one station is the center of the town of Lixouri (City Hall building) whereas the location of the 2nd station in the old school of the village of Chavriata. As could be observed in figure 7 the church of Agia Marina at Sullaroi is at a distance of approximately 2km from either the Lixouri or the Chavriata station located between these two locations. The church of Panagia of Roggoi is at a distance of approximately 5km North from Chavriata and North-West from Lixouri. In order to obtain an estimate of the horizontal seismic forces that these two churches were subjected to during the damaging aftershock of 3rd of February 2015 the constant ductility ($\mu=1.5$) response spectra in the East-West and North-South direction were derived from those recordings of the ground motion. The corresponding response spectral curves are depicted in figures 17 and 18 for the Lixouri recording and in figures 19 and 20

for the Chavriata recording in the East-West and North-South horizontal directions, respectively.

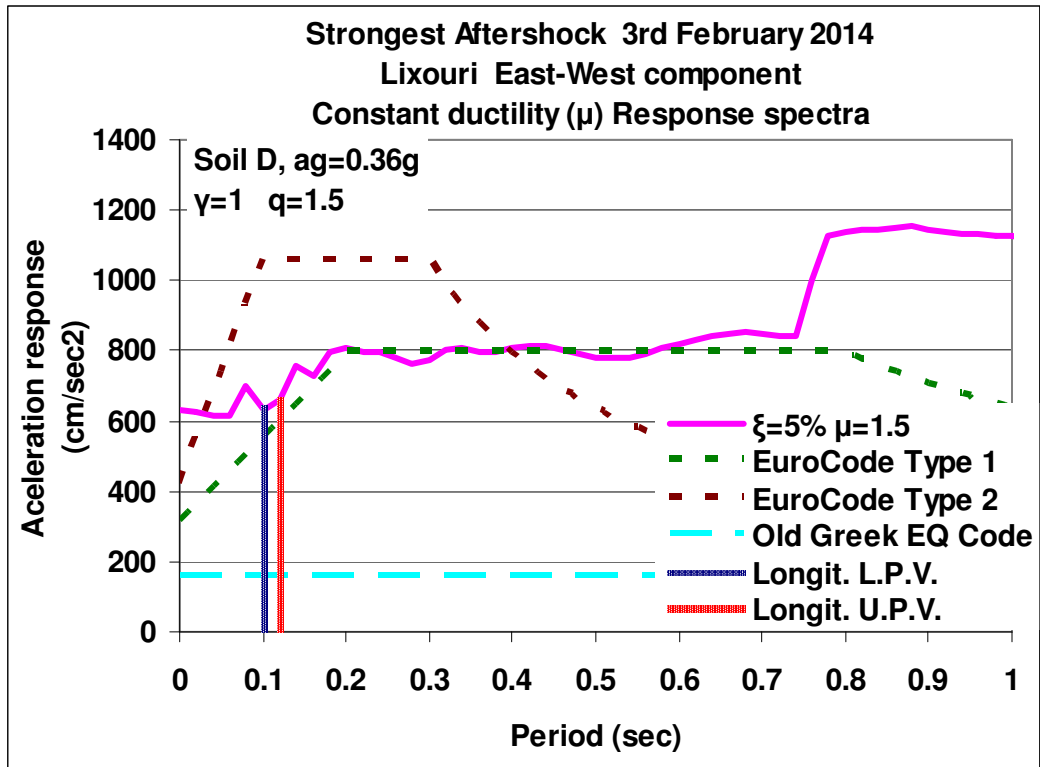


Figure 17. Definition of East-West (y-y) seismic loads through the recorded ground motion at Lixouri during the 3rd of February strongest aftershock

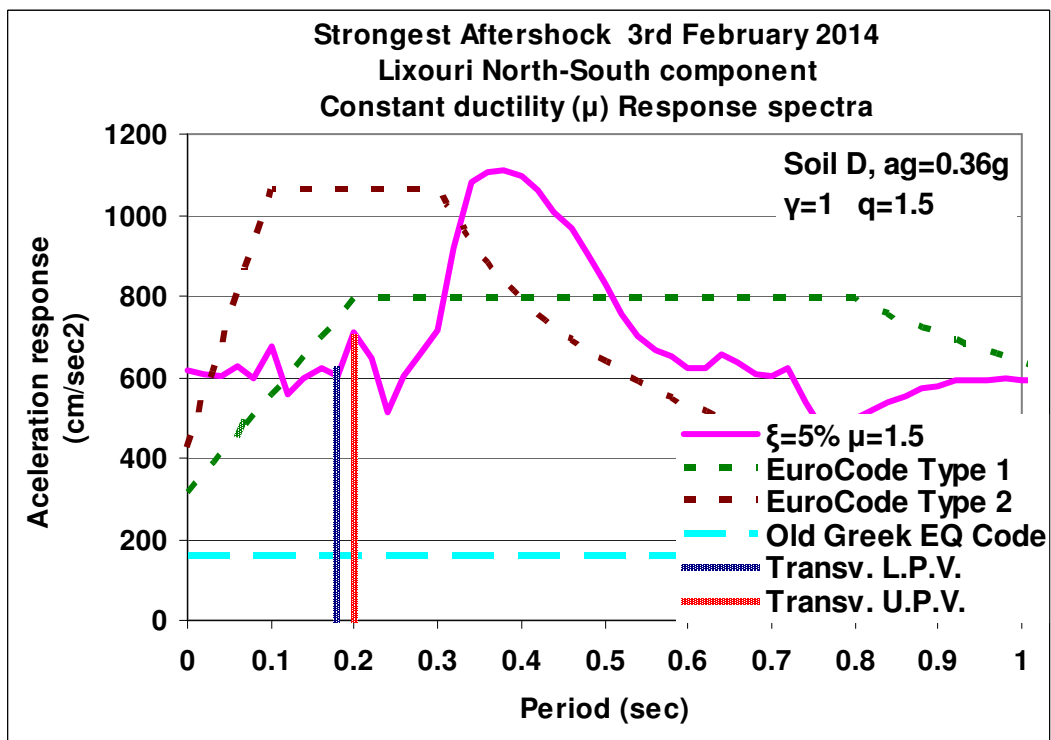


Figure 18. Definition of North-South (x-x) seismic loads through the recorded ground motion at Lixouri during the 3rd of February strongest aftershock

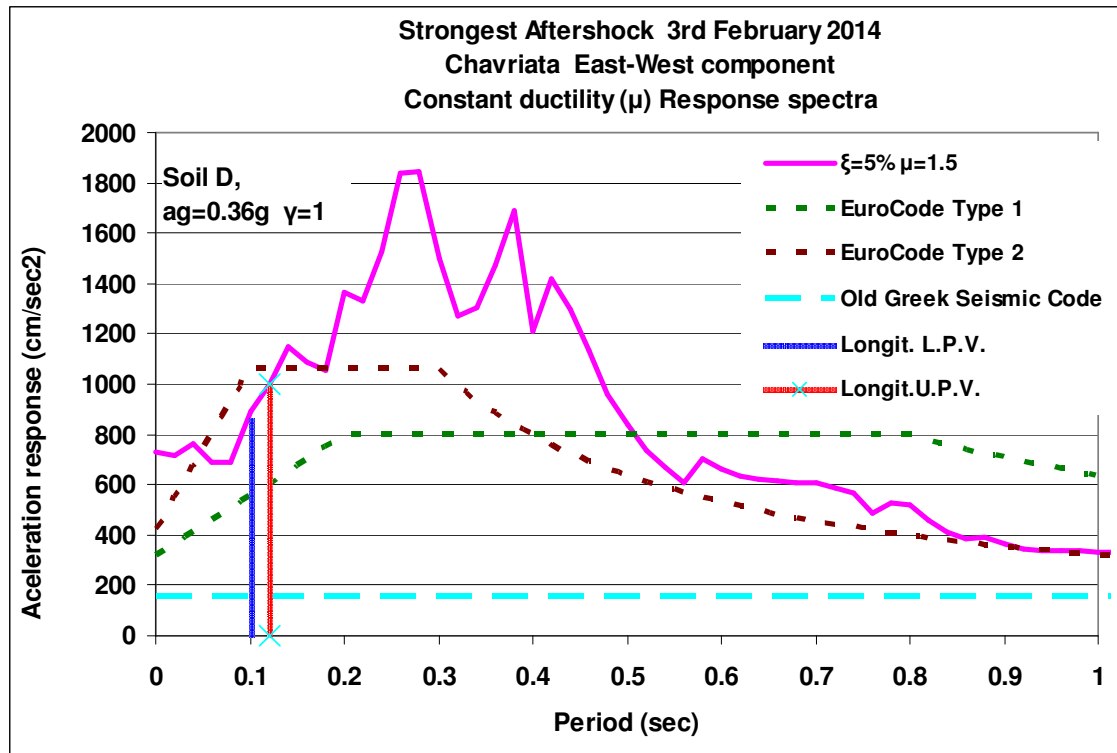


Figure 19. Definition of East-West (y-y) seismic loads through the recorded ground motion at Chavriata during the 3rd of February strongest aftershock

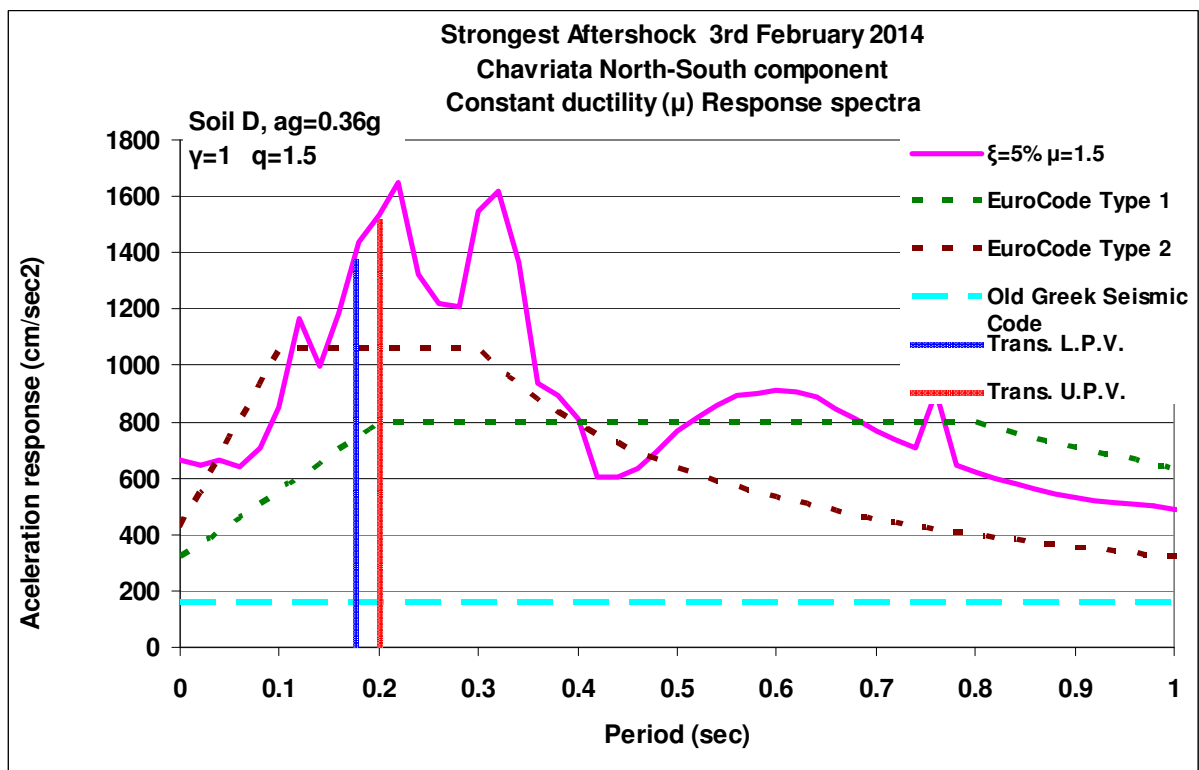


Figure 20. Definition of North-South (x-x) seismic loads through the recorded ground motion at Lixouri during the 3rd of February strongest aftershock

The ductility factor value $\mu=1.5$ is presumed to be a good approximation for these type of relatively brittle unreinforced masonry construction. In the same figures the design spectral

acceleration curves are also plotted for type 1 and type 2 earthquake, as these design spectral values are defined by EuroCode part 8 [24] assuming again a response modification factor value $q=1.5$ Soil category D (flexible soil) importance factor 1 and design peak ground acceleration equal to $0.36g$ (g the acceleration of gravity) as defined by the current Greek seismic code for Kefalonia [25]. In comparison, the “Old Greek Seismic Code” level of seismic forces that were introduced in 1959 are also indicated in this figure as “Old Greek Seismic Code” [5]. Moreover, the values of the eigen-periods found from the dynamic analyses of these two churches, as they were presented in figures 15 and 16 are also plotted in figures 17 to 20. These values are designated as Longit. L.P.V or U.P.V., which correspond to the eigen-periods in the longitudinal East-West (x-x) direction for either the hard soil (Lower Period Value) or the medium soil (Upper Period Value). The same hold for the transverse North-South (y-y) direction which are designated as Trans. L.P.V or U.P.V., for the hard soil (Lower Period Value) or the medium soil (Upper Period Value), respectively. The following remarks can be made on the basis of figures 17 to 20.

- 1) For the period range from 0.1sec. to 0.4sec the Chavriata spectral acceleration curve would result in more demanding seismic forces for the corresponding structures, like the studied churches, than the Lixouri spectral acceleration curve for both the North-South and the East-West directions.
- 2) Structural systems that would be more flexible than the ones examined here, either because of more flexible soil-foundation conditions than the medium soil of this study or for more flexible structures themselves than the structures considered here, they would have been subjected to larger horizontal seismic forces than the ones to be considered for the studied here churches. This remark is valid for the Chavriata record for both the North-South and East-West direction and for the East-West direction for the Lixouri record.
- 3) The Chavriata spectral acceleration curves (for $\mu=1.5$ either E-W or N-S) for the period range from 0.1sec. to 0.4sec would result in more demanding seismic forces for the corresponding structures, like the churches studied here, than the EuroCode 8 design spectral curves for $q=1.5$.
- 4) The Lixouri spectral acceleration curve (for $\mu=1.5$ either N-S or E-W) for the period range from 0.1sec. to 0.4sec would result in less demanding seismic forces for the corresponding structures, like the churches studied here, than the Type 1 EuroCode 8 design spectral curves for $q=1.5$. The difference is not very significant for the type 2 EuroCode 8 design spectral curves for $q=1.5$. The
- 5) Seismic force levels for the period range from 0.1sec. to 0.4sec according to the old Greek seismic code are approximately 3 to 4 times smaller than the corresponding levels obtained on the basis of the Lixouri spectral curves (for $\mu=1.5$ either E-W or N-S) or the type 2 EuroCode 8 design spectral curves for $q=1.5$.
- 6) Seismic force levels for the period range from 0.1sec. to 0.4sec according to the old Greek seismic code are approximately 5 to 6 times smaller than the corresponding levels obtained on the basis of the Chavriata spectral curves (for $\mu=1.5$ either E-W or N-S) or the type 2 EuroCode 8 design spectral curves for $q=1.5$.
- 7) All the previous points underline the severity of seismic forces levels the examined churches had to withstand. One favourable parameter for the structural performance was the short duration of this intense shaking. However, the preceding discussion on the severity of the seismic forces ignored the unfavourable effect of the vertical component of the ground motion, which is usually present in localities close to the epicen-

ter like the ones examined here. This unfavourable influence of the vertical component of the ground motion is ignored throughout this study.

The seismic forces that are used in this type of numerical analyses are obtained in the following way.

- First, employing either the Lixouri or the Chavriata spectral curves for $\mu=1.5$ and the linear elastic numerical simulation of the examined structural system the base shear values in the North-South or the East-West direction are obtained. This is done through a dynamic spectral analysis utilizing the first four (4) eigen-modes and the relevant North-South or East-West spectral curves, respectively. Alternatively, a response spectrum can be used resulting from the elastic response spectral curve for 5% damping divided by a response modification factor equal to 1.5 for unreinforced masonry. In the subsequent analysis the later process was adopted.
- An amplification factor is also utilized to compensate for the fact that these first four (4) eigen-modes, which correspond to realistic structural responses for this type of structures, do not sum up to 90% of the total mass of the structure.
- The horizontal seismic forces are finally applied either in the x-x East-West longitudinal direction (E_x) or the y-y North-South transverse direction (E_y) as static forces resulting from constant acceleration along the height of the examined structures as shown in figure 21. This constant acceleration has such a value that results in the same base shear value found from the dynamic spectral analysis of steps a and b described before. These equivalent seismic forces E_x or E_y are combined with the permanent loads (D) to form the load combinations $0.9D \pm E_x$ or $0.9D \pm E_y$.
- This is done because it is much easier to obtain in this way the demands of the various masonry structural elements from the seismic forces described in step c. Thus, the evaluation of the seismic performance of these structural elements can be done.

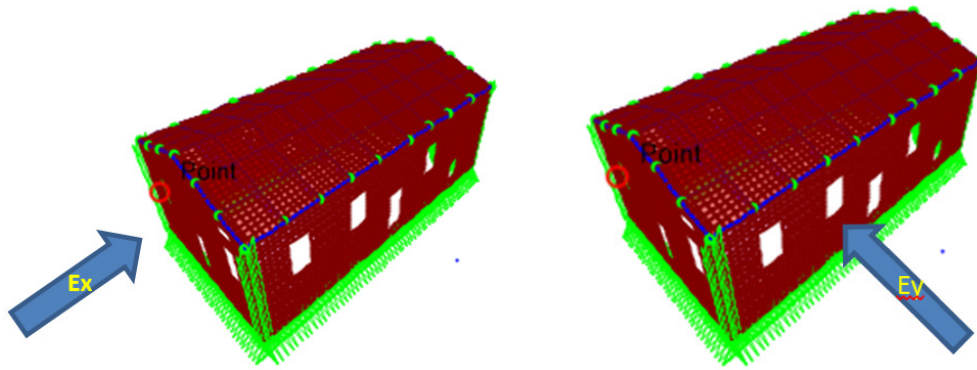


Figure 21: Equivalent static loads.

Table 3	<i>Base shear Values (KN) based on the Chavriata response spectra</i>			
	Virgin Mary of Roggoi Hard Soil	Virgin Mary of Roggoi Soft Soil	Ag. Marina Soullaroi Hard Soil	Ag. Marina Soullaroi Soft Soil
North-South (x-x) direction	2465	2498	5229	5803
East-West (y-y) direction	2367	2874	8397	8828

Table 3 lists the base shear values, as they resulted from the linear elastic dynamic spectral analyses utilizing the East-West or North-South acceleration response spectral curves for 5% damping and $q=1.5$ derived from the recorded ground acceleration (figures 17 to 20). As explained above, these values coincide with the equivalent seismic forces E_x or E_y .

4.2 Push-over numerical analyses with non-linear mechanisms for the two-node links at the foundation-soil interface and the link elements which connect the vertical walls in the corners and the top face of the wall with the roof.

In the 2nd category of numerical seismic analyses the non-linear behaviour of the examined structures is considered by introducing the following non-linear mechanisms.

a1) First, the two-node 3-D links at the soil-foundation interface introduced to account for the soil-foundation deformability are provided with tension a cut-off limit so they can sustain only compression in their axial direction and no tension.

b1) Similarly, two-node 3-D non-linear link elements are also utilized in connecting the vertical walls at their corners with a tension cut-off limit in a way to transfer compression between the intersecting walls at the corner but limit transfer of tension.

c1) A similar connection is used between the wooden elements of the roof and the tympana of the masonry walls at the East and West sides or at the top of the North or South longitudinal masonry walls.

Thus, through the proper use of these non-linear 3-D two-node link elements these non-linear mechanisms are introduced in an effort to simulate numerically the capability of the uplifting of the structure at the soil-foundation interface, the possibility of detachment between the wooden elements of the roof and the masonry walls or between the vertical walls themselves at the corners.

These numerical analyses were a push-over step-by-step type of analyses [6] with the first step being the application of the permanent vertical loads (D). Next, the horizontal seismic loads are introduced at each shell element (each mass) as a gravity load at direction either in the North-South (y-y) or East-West (x-x) directions. This is done gradually by increasing the level of the applied seismic forces by a small amount at each subsequent step. The seismic horizontal displacement attained at each step is checked certainly at the top point of East wall for the East-West (x-x) push-over analyses or at the top of the middle of the North wall for the push-over analyses direction in the North-South (y-y) direction.

5 ASSUMED FAILURE CRITERIA USED IN THE VALUATION OF THE OBSERVED PERFORMANCE

Table 4 lists the assumed mechanical characteristics for the stone masonry elements of both churches [5]. Moreover, a Mohr-Coulomb failure envelope was adopted for the in-plane shear limit state of the stone masonry, when a on normal stress is acting simultaneously, that is defined through the relationship (1) ([6], [21], [26]).

$$f_{vk} = f_{vko} + 0.4 \sigma_n \quad (1)$$

where: f_{vko} is the shear strength of the stone masonry when the normal stress is zero; f_{vko} was assumed to be equal to 0.160 N/mm². σ_n is the compressive axial stress acting on the bed joint .

Table 4 lists the assumed mechanical characteristics for the stone masonry in terms of Young's modulus and Poisson's ratio as well as compressive and tensile strength values. The values listed in table 4 were assumed to be valid for both churches based on relevant strength values employed in similar studies [6 to 21]. However, the necessity to quantify such limit value through tests based on in-situ samples must once more be underlined.

Table 4. Assumed Mechanical Characteristics of the Stone Masonry

	Young's Modulus (N/mm ²)	Poisson's Ratio	Compressive Strength (N/mm ²)	Tensile Strength normal /parallel bed-joint (N/mm ²)	shear strength f_{vko} (N/mm ²)
Limit values	1000	0.2	3.50	0.15 / 0.60	0.16

The above strength values will be used to evaluate the seismic performance of the various masonry structural elements in the most critical locations that the demands, obtained through the numerical analyses results, have maximum values. This will be done in comparing the various demands S_{Ed} with the corresponding strengths S_{Rd} through the following inequality (2):

$$S_{Ed} < S_{Rd} \quad \text{indicates safe structural performance.} \quad (2)$$

The above inequality can also have the form of a S_{Rd} / S_{Ed} in inequality (3).

$$S_{Rd} / S_{Ed} > 1 \quad \text{indicates safe structural performance.} \quad (3)$$

This inequality in ratio terms is further detailed through the following ratios. For the in-plane or the out of plane demands the following demands are checked (inequalities 4 to 6):

a2) The in-plane shear demand in terms of shear stress for various bed-joint locations where shear and normal stresses are acting. This is done through the value of the following ratio R_τ

$$R_\tau = \text{shear strength} / \text{shear stress demand} < 1 \quad \text{signifies shear failure (in-plane)} \quad (4)$$

b2) The in-plane compression stress demand for various bed-joint locations where compressive stresses are acting normal to bed-joints. This is done through the value of the following ratio R_ζ

$$R_\zeta = \text{compressive strength} / \text{compressive stress demand} < 1 \quad \text{signifies compression failure (in-plane)} \quad (5)$$

c2) The in-plane tensile stress demand for various bed-joint locations where tensile stresses are acting normal to bed-joints. This is done through the value of the following ratio R_σ

$$R_\sigma = \text{tensile strength (fxk1)} / \text{tensile stress demand} < 1 \quad \text{signifies tensile failure normal to bed joint (in-plane)} \quad (6)$$

d2) The out-of-plane tensile stress demand for various bed-joint locations where tensile stresses are acting normal to bed-joints. This is done through the value of the following ratio R_M

$R_M = \text{tensile strength} / \text{tensile stress demand from out-of-plane flexure} < 1$ signifies out-of-plane tensile failure normal to bed joint at the extreme fiber (out of plane) (7)

All the masonry parts of the studied structures were examined in terms of in-plane and out-of-plane stress demands posed by the considered load combinations against the corresponding capacities, as these capacities were obtained by applying the Mohr-Coulomb criterion of equation 1 or the stone masonry compressive and tensile strength limits listed in Table 4. Ratio values smaller than one (R_τ , R_ζ , R_σ , $R_M < 1$) predict a corresponding limit state condition. As can be seen, the followed methodology is based on combining numerical stress demands resulting from elastic analyses with limit-state strength values. A different approach is to incorporate these limit-state strength values in a non-linear push-over type of analysis (see Manos et al. [1]). It was shown that the methodology applied here correlates quite well with the non-linear approach in predicting regions of structural damage.

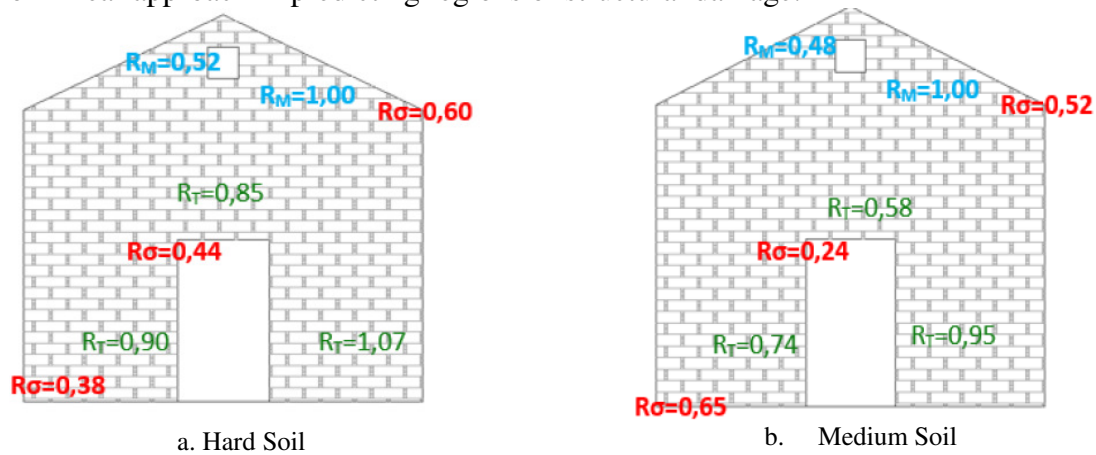


Figure 22. Predicted performance of the West side wall of the church of Panagia of Roggoi



Figure 23. Observed damage of the West side of the church Panagia of Roggoi

6 THE RESULTS OF THE NUMERICAL ANALYSES

Next, selected results from the numerical simulations of the earthquake response of these two churches are presented. The numerical analyses results obtained following the linear static approach, described in sub-section 4.1, are presented first in sub-section 6.1. This is done by showing the predicted performance of the various masonry elements utilizing the obtained demands with the corresponding strength values through the process outlined in section 5. Selected results obtained through the push-over type of numerical analyses, described in sub-section 4.2, are next presented in a summary form in sub-section 6.2.

6.1 Static numerical analyses with linear mechanisms for the two-node links at the foundation-soil interface as well as at the corner of masonry wall interconnections.

Figures 22a and 22b depict R_t , R_σ , R_M ratio values for the in-plane and out-of-plane performance of the West side of the Panagia of Roggoi church for either hard or medium soil, respectively. As can be seen in these figures the demands exceed by far the corresponding strengths either in shear or tension (in-plane) at the lower part of this masonry wall or the out-of-plane tension at its upper part. The presence of medium soil signifies that these ratio values become in general even smaller. Thus, it is demonstrated that the presence of medium soil conditions increases the possibility of damage in this case. Good agreement can be seen by comparing the predicted (figures 22) with the observed (figure 23) performance for this wall.

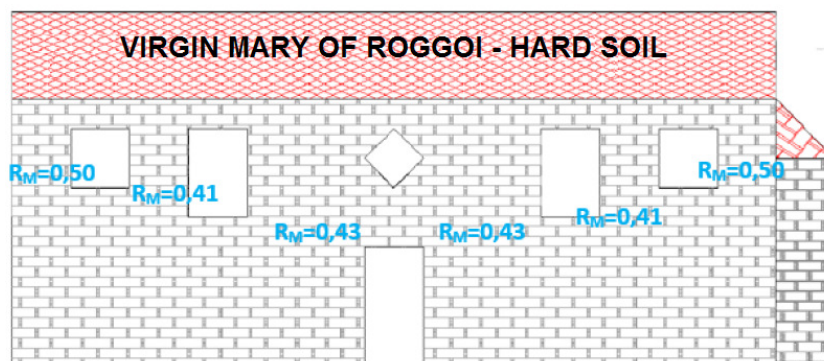


Figure 24a. Predicted out-of-plane performance, South wall, hard soil, church Panagia of Roggoi

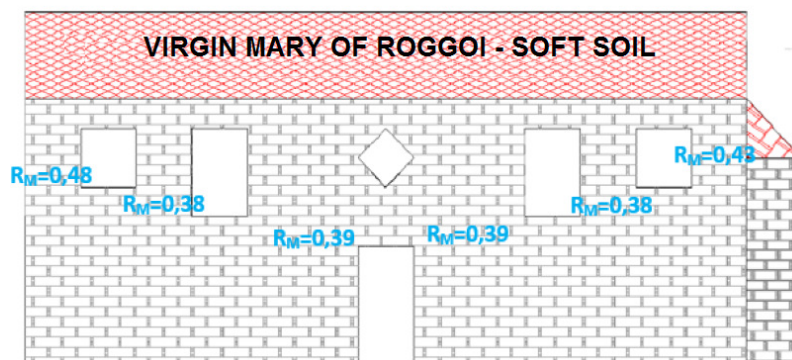


Figure 24b. Predicted out-of-plane performance, South wall, medium soil, church Panagia of Roggoi

Figures 24a and 24b depict R_M ratio values for out-of-plane predicted performance of the South side of the Panagia of Roggoi church for either hard or medium soil, respectively. As can be seen in these figures the demands exceed by far the corresponding strengths in tension (out-of-plane) at the upper part of this masonry wall between the door and window openings.

Again, the presence of medium soil signifies that these ratio values become in general even smaller. Thus, it is demonstrated that the presence of medium soil conditions increases the possibility of damage in this case. Good agreement can be seen again by comparing the predicted (figures 24) with the observed (figure 25) performance for this wall.



Figure 25. Observed out-of-plane performance, South wall, church Panagia of Roggoi

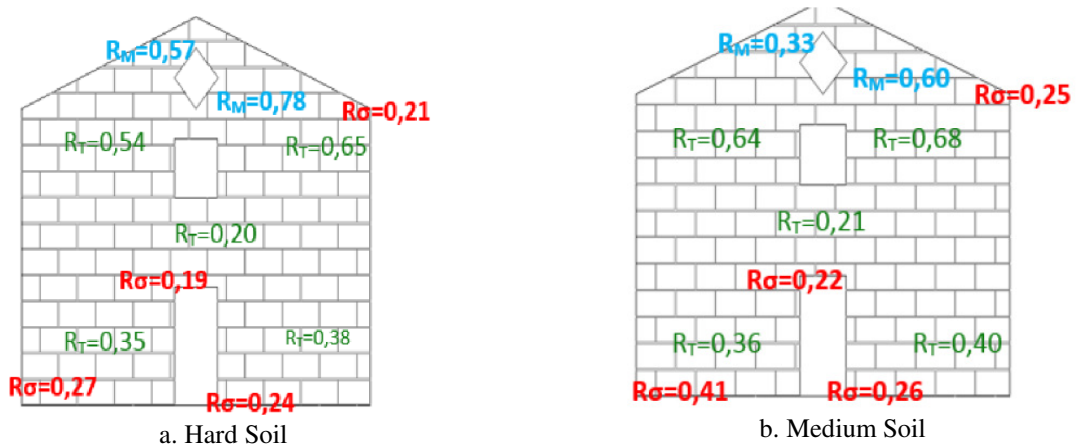


Figure 26. Predicted performance of the West side wall of the church of Agia Marina



Figure 27. Observed damage of the West side of the church of Agia Marina

Figures 26a and 26b depict R_t , R_σ , R_M ratio values for the in-plane and out-of-plane performance of the West side of the Agia Marina church for either hard or medium soil, respectively. As can be seen in these figures the demands exceed by far the corresponding strengths either in shear or tension (in-plane) at the lower part of this masonry wall or the out-of-plane tension at its upper part. The presence of medium soil signifies that these ratio values become in general even smaller. Thus, it is demonstrated that the presence of medium soil conditions increases the possibility of damage in this case. Good agreement can be seen by comparing the predicted (figures 26) with the observed (figure 27) performance for this wall.

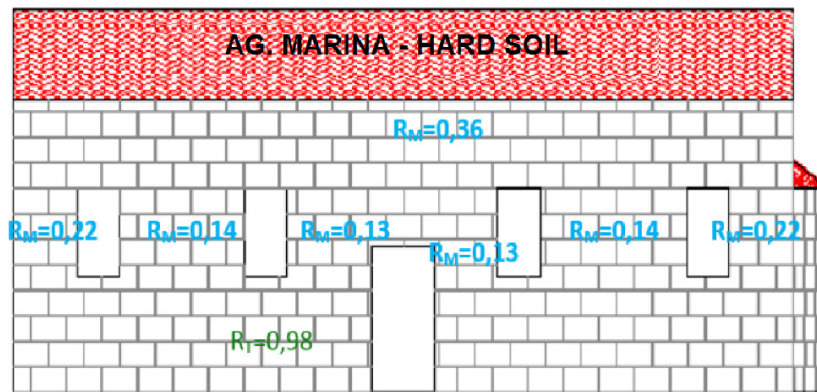
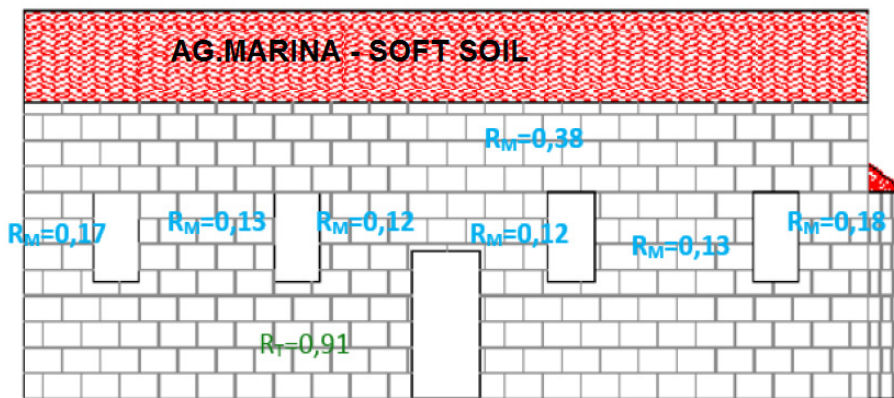


Figure 28a. Predicted out-of-plane performance, South wall, hard soil, church Agia Marina



28b. Predicted out-of-plane performance, South wall, medium soil, church Agia Marina



Figure 29. Observed out-of-plane performance, South wall, church Agia Marina

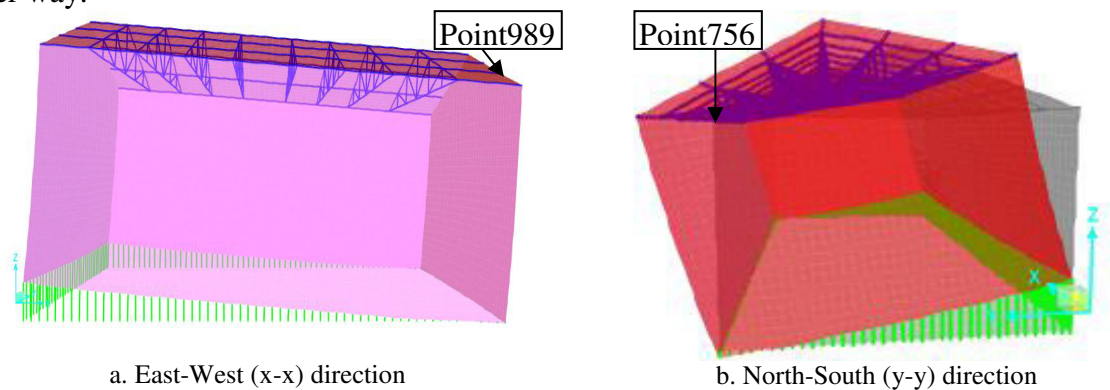
Figures 28a and 28b depict R_M ratio values for out-of-plane predicted performance of the South side of the Agia Marina church for either hard or medium soil, respectively. As can be seen in these figures the demands exceed by far the corresponding strengths in tension (out-of-plane) at the upper part of this masonry wall between the door and window openings. Again, the presence of medium soil signifies that these ratio values become in general even smaller. Thus, it is demonstrated that the presence of medium soil conditions increases the possibility of damage in this case. Good agreement can be seen again by comparing the predicted (figures 28) with the observed (figure 29) performance for this wall.

7 RESULTS FROM THE PUSH-OVER NUMERICAL ANALYSES

Next, selected results from the push-over numerical simulations of the earthquake response of this type of churches are presented.

7.1 The uplifting of the foundation.

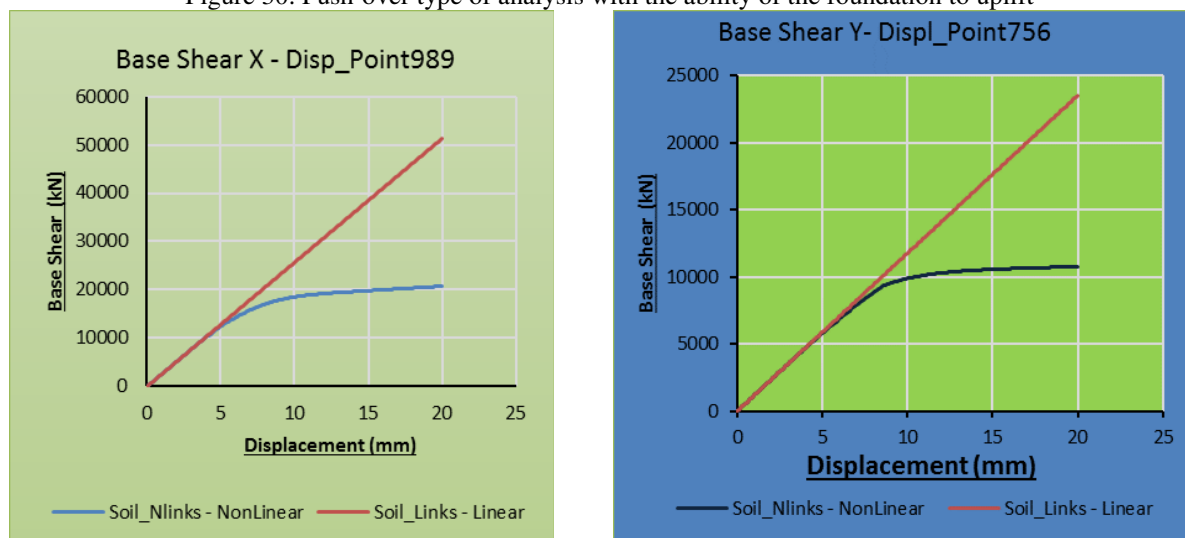
Figures 30a and 30b depict the push-over displacement response as predicted from the numerical simulations that included the 1st non-linear mechanism, that of the ability of the foundation to uplift from the foundation-soil interface, when the loads combinations $0.9D + E_x$ or $0.9D + E_y$, with the seismic forces E_x (East-West) or E_y (North-South), are applied in a push-over way.



a. East-West (x-x) direction

b. North-South (y-y) direction

Figure 30. Push-over type of analysis with the ability of the foundation to uplift



a. East-West (x-x) direction

b. North-South (y-y) direction

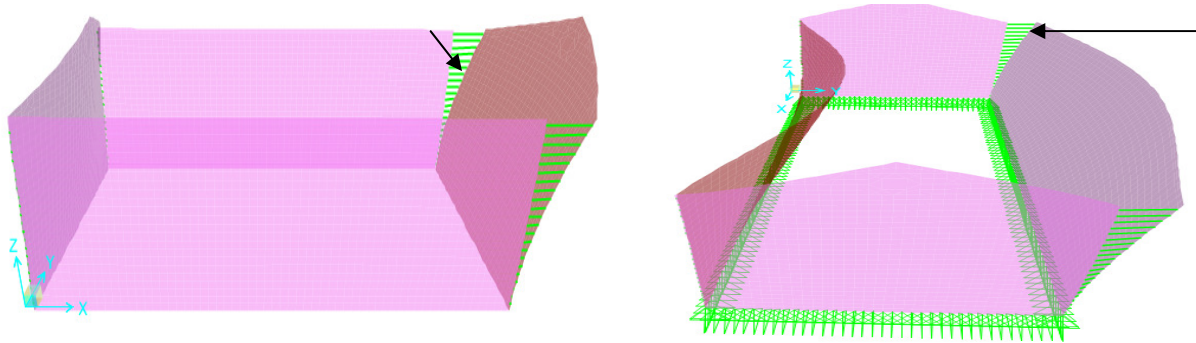
Figure 31. Base-shear versus top horizontal displacement Push-over response with foundation uplift

The obtained base shear – horizontal displacement response from these push-over numerical analyses are depicted in figures 31a (0.9D + Ex) and 31b (0.9D + Ey) for the East-West and North-South directions, respectively.

As can be seen in figures 31a and 31b the uplifting of the foundation limits the base shear levels in the East-West direction to approximately 12000KN and in the North-South direction approximately 9000KN. If the above values are compared with the corresponding values, listed in Table 3, which were obtained from the dynamic spectral analyses that employed the recorded ground motion response spectra (Chavriata record), it can be concluded that for these force levels the uplifting of the foundation is unlikely.

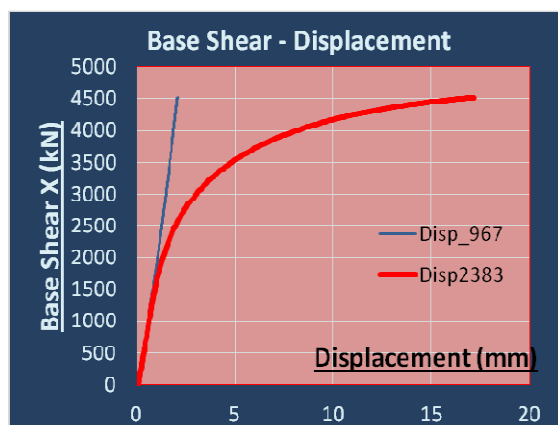
7.2 The detachment of the walls at the corners.

Figures 32a and 32b depict the push-over displacement response as predicted from the numerical simulations that included the 2nd non-linear mechanism, that of the ability of the walls to be detached at the corners where these vertical walls are interconnected. This is simulated when the load combinations 0.9D + Ex or 0.9D + Ey, with the seismic forces Ex (East-West) or Ey (North-South) are applied in a push-over way.

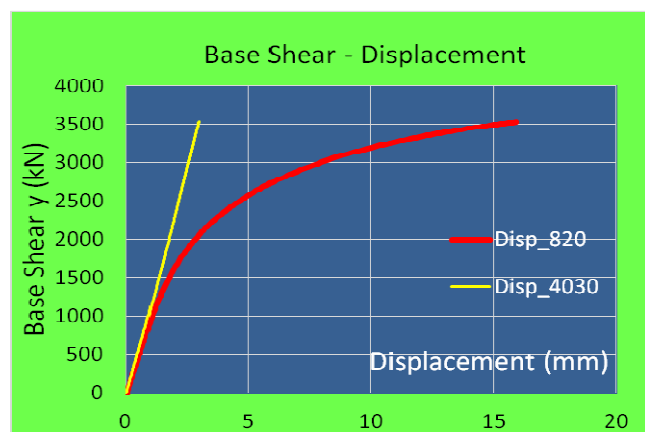


a. East-West (x-x) direction – detachment of East wall from the North wall b. North-South (y-y) direction – detachment of North wall from West wall

Figure 32. Push-over type of analysis with the ability of the foundation to uplift



a. East-West (x-x) direction – detachment of the East wall from the North wall



b. North-South (y-y) direction – detachment of the North wall from the West wall

Figure 33. Base-shear versus top horizontal displacement Push-over response with the ability of the vertical walls to be detached at the corners

The obtained base shear – horizontal displacement response from these push-over numerical analyses are depicted in figures 33a (0.9D + Ex) and 33b (0.9D + Ey) for the East-West

and North-South directions, respectively. As can be seen in figures 32a and 33a the detachment of the East wall from the North wall, when the seismic forces act in the East-West direction, limits the base shear levels in the East-West direction to approximately 4000KN. Similarly, the detachment of the North wall from the West wall (figures 32b and 33b), when the seismic forces act in the North-South direction, limits the base shear at the level of approximately 3500KN. If the above values are compared with the corresponding values, listed in Table 3, which were obtained from the dynamic spectral analyses that employed the recorded ground motion response spectra (Chaviata record), it can be concluded that for these force levels the detachment of these walls at the corners is very likely.

7.3 The detachment of the walls at the corners as well as at the roof level.

Figures 34a and 34b depict the push-over displacement response as predicted from the numerical simulations that included the 2nd and the 3rd non-linear mechanisms; that is the ability of the walls to be detached at the corners where these vertical walls are interconnected as well as at the roof level. This is simulated when the load combinations $0.9D + E_x$ or $0.9D + E_y$, with the seismic forces E_x (East-West) or E_y (North-South) are applied in a push-over way.

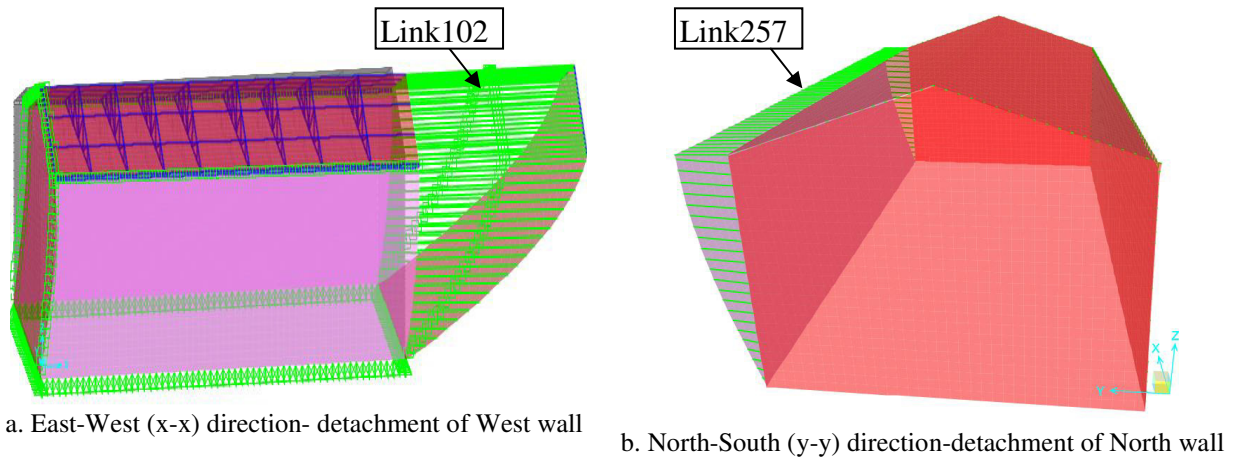


Figure 34. Push-over type of analysis with the ability of the walls to be detached at the corners

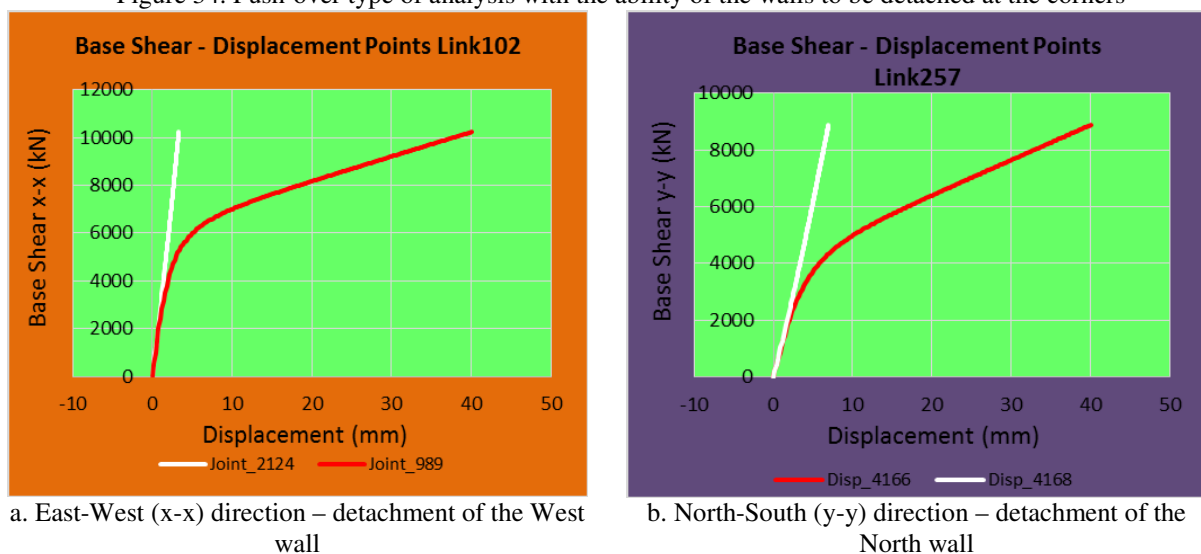


Figure 35. Base-shear versus top horizontal displacement Push-over response with foundation uplift

The obtained base shear – horizontal displacement response from these push-over numerical analyses are depicted in figures 35a (0.9D + Ex) and 35b (0.9D + Ey) for the East-West and North-South directions, respectively. As can be seen in figures 33a and 33b the detachment of the West wall limits the base shear levels in the East-West direction to approximately 6000KN and in the North-South direction approximately 5000KN. If the above values are compared with the corresponding values, listed in Table 3, which were obtained from the dynamic spectral analyses that employed the recorded ground motion response spectra (Chavriata record), it can be concluded that for these force levels the detachment of these walls at the corners is very likely. These are in agreement with the observed performance (see figures 13 and 14).

8 CONCLUSIONS

- Through the systematic study of the characteristics of the ground motion records and the dynamic properties of the structural systems, representing the examined Christian churches damaged in Kefalonia by the 3rd of February 2015 strongest aftershock, the levels of the seismic forces and their severity that these churches had to withstand was established. One favourable parameter for the structural performance was the short duration of this intense shaking. However, this study ignored the unfavourable effect of the vertical component of the ground motion, which is usually present in localities close to the epicenter like the ones examined here.
- The predicted performance of the examined Christian churches, employing demands from a linear analysis that utilizes these horizontal seismic force levels and assumed strength values for stone masonry, yield good agreement with the observed performance.
- The predicted performance is approximated through a detailed process that makes use of strength / demand ratio values (R_τ , R_ζ , R_σ , R_M) in order to approximate the ability of the masonry structural elements to withstand or not the posed demands in in-plane shear, in-plane compression/tension and out-of-plane tension.
- The push-over non-linear numerical analyses that were next performed including the ability of foundation uplift and the ability of the walls to be detached from their interconnections at the corners or at their connection with the roof seems to yield realistic estimates of the observed performance.

REFERENCES

- [1] GEER - EERI - ATC - Cephalonia GREECE *Earthquake Reconnaissance January 26th/ February 2nd 2014 Version 1: June 6 2014*
- [2] Institute of Geodynamics-National Observatory of Athens-Greece, “The earthquake sequence of January-February 2014 in Kefalonia-Greece”, Draft report of , Athens 20th February, 2014.
- [3] Ch. Papaioannou et al. “Strong ground motion of the 3rd February 2014, (M=6.0) Kefalonia Earthquake”, Institute of Earthquake Engineering and Engineering Seismology Report, February, 2014.
- [4] Papazachos, B. and Papazachou, K., 1989, 1997, 2003. The earthquakes of Greece, *Zitis Publ.,Thessaloniki*, 356 pp., 304 pp., 286 pp. (in Greek).

- [5] G.C. Manos, Seismic Code of Greece, Chapter 17, International Handbook of Earthquake Engineering: "Codes, Programs and Examples", *edited by Mario Paz, by Chapman and Hall*, ISBN 0-412-98211-0, 1994.
- [6] G.C. Manos, V.J. Soulis, A. Diagouma, "Numerical Investigation of the behaviour of the church of Agia Triada, Drakotrypa, Greece", *Advances in Engineering Software*, Vol. 39/4, pp 284-300, 2007.
- [7] G.C. Manos, V.J. Soulis, O. Felekidou, "The dynamic and Earthquake Behavior of Greek Post-Byzantine Churches", 14WCEE, Beijing, CHINA, 2008.
- [8] G. C. Manos, V. J. Soulis, O. Felekidou, A. Koutsianou, P. Lipiridou, «The dynamic and earthquake response of Greek Byzantine and Post-Byzantine Basilicas», COMDYN 2009, Rhodes, Greece.
- [9] G.C Manos, V. Soulis, N. Karamitsios, O. Felekidou, Numerical Simulation of the Dynamic and Earthquake Behaviour of Greek Post-Byzantine Churches with and without Base Isolation", PROHITECH 2009, 21 to 24 June 2009, Rome, Italy..
- [10] Manos George, Soulis V., Felekidou O., Karamitsios N., Kotoulas L., "Dynamic and Seismic Behavior of Greek Post-Byzantine Churches with or without Base Isolation", 8th International Masonry Conference, 2010, Dresden, Germany.
- [11] Manos George, Soulis V., Felekidou O., "Numerical Study of the Dynamic and Earthquake Behavior of Byzantine and Post-Byzantine Basilicas", 8th International Masonry Conference, 2010, Dresden, Germany.
- [12] Manos George, Soulis V., Felekidou O., Matsou V. "A Numerical Investigation of the Dynamic and Earthquake Behavior of Byzantine and Post-Byzantine Basilicas", 9th U.S. National and 10th Canadian Earthquake Engineering Conference, 2010, Toronto, Canada.
- [13] G. C. Manos, V. Soulis, O. Felekidou, N. Karamitsios, L. Kotoulas, "Numerical Study of the Dynamic and Earthquake Response of Greek Post-Byzantine Churches with or without Base Isolation", 3rd International Workshop on Conservation of Heritage Structures Using FRM and SHM, 2010, Ottawa, Canada.
- [14] Manos George, Soulis V., Felekidou O., Matsou V. "A Numerical Investigation of the Dynamic and Earthquake Behavior of Byzantine and Post-Byzantine Basilicas", 3rd International Workshop on Conservation of Heritage Structures Using FRM and SHM, 2010, Ottawa, Canada.
- [15] G.C. Manos, N. Karamitsios, " Numerical Simulation of the Dynamic and Earthquake Behavior of Greek Post-Byzantine Churches with and without Base Isolation", COMPDYN 2011, Corfu, Greece, 26–28 May 2011.
- [16] G.C. Manos, N. Karamitsios, "Study of the Dynamic and Earthquake Response of Greek Post-Byzantine Churches with and without Base Isolation" EURODYN 2011, Leuven, Belgium, 4-6 July, 2011.
- [17] G. C. Manos and N. Karamitsios, "Earthquake Numerical Simulation of the Dynamic and Earthquake Behaviour of Greek Post-Byzantine Churches with and without Base Isolation", STREMAH-2011, Chianciano, Italy, Sep. 2011.
- [18] Manos George, "Consequences on the urban environment in Greece related to the recent intense earthquake activity", *Int. Journal of Civil Engineering and Architecture*, Dec. 2011, Volume 5, No. 12 (Serial No. 49), pp. 1065–1090.

- [19] G. C. Manos, V. J. Soulis & N. Karamitsios, “The Performance of Post-Byzantine churches during the Kozani-1995 Earthquake – Numerical Investigation of their Dynamic and Earthquake Behavior”, 15WCEE, (2012) Portugal.
- [20] G. C. Manos & N. Karamitsios , “Numerical simulation of the dynamic and earthquake behavior of Greek post-Byzantine churches with and without base isolation”, Earthquake Engineering Retrofitting of Heritage Structures, Design and evaluation of strengthening techniques, pp. 171-186, Edited By: S. Syngellakis, Wessex Institute of Technology, UK, ISBN: 978-1-84564-754-4, eISBN: 978-1-84564-755-1, 2013.
- [21] G.C. Manos, L. Kotoulas, V. Matsou, O. Felekidou, “Dynamic behaviour of Greek Post-Byzantine churches with foundation deformability and evaluation of their earthquake performance”, 4th ECOMASS Thematic Conference on Computational Methods in Structural Dynamics and Earthquake Engineering – COMPDYN 2013, 12-14 June 2013, Kos Island, Greece.
- [22] G.C. Manos and E. Kozikopoulos, “In-situ measured dynamic response of the bell tower of Agios Gerasimos in Lixouri-Kefalonia, Greece and its utilization in the numerical predictions of its earthquake response”, *CompDyn 2015 to be published*.
- [23] G.C. Manos, D. Naxakis, V. Soulis, “The Dynamic and earthquake response of a two-story old R/C building with masonry infills in Lixouri-Kefalonia Greece, including soil-foundation deformability”, *CompDyn 2015 to be published*.
- [24] Eurocode 8: Design of structures for earthquake resistance - Part 1: General rules, seismic actions and rules for buildings, *FINAL DRAFT prEN 1998-1, December 2003*.
- [25] Provisions of Greek Seismic Code 2000 , EPPO, Earthquake Planning and Protection Organization Athens, Greece, December 1999.
- [26] Eurocode 6 part 1: Design of structures for earthquake resistance - Part 1: General rules, seismic actions and rules for buildings, *FINAL DRAFT prEN 1998-1, December 2003*.